ture. It is now possible to obtain well-characterized, highly purified SWNT materials that are suitable for physical property measurements. Soluble SWNTs are versatile precursors to copolymer materials with distinctive mechanical and electrical properties and as new ligands for metal complexation.

References and Notes

1. B. I. Yakobson and R. E. Smalley, *Am. Sci.* **85**, 324 (1997).
2. A. Thess *et al.*, *Science* **273**, 483 (1996).
3. C. Journet *et al.*, *Nature* **388**, 756 (1997).
4. Y. Chen *et al.*, *J. Mater. Res.* **13**, 2423 (1998).
5. J. Liu *et al.*, *Science* **280**, 1253 (1998).
6. A. M. Rao *et al.*, *ibid.* **275**, 187 (1997).
7. S. Bandow *et al.*, *Phys. Rev. Lett.* **80**, 3779 (1998).
8. R. C. Haddon, *Nature* **378**, 249 (1995).
9. _____, *ibid.* **388**, 31 (1997).
10. A. M. Rao, P. C. Eklund, S. Bandow, A. Thess, R. E. Smalley, *ibid.*, p. 257.
11. J. W. G. Wildoer, L. C. Venena, A. G. Rinzler, R. E. Smalley, C. Dekker, *ibid.* **391**, 59 (1998).
12. T. W. Odom, J.-L. Huang, P. Kim, C. H. Lieber, *ibid.*, p. 62.
13. T. Pichler *et al.*, *Phys. Rev. Lett.* **80**, 4729 (1998).
14. R. S. Lee, H. J. Kim, J. E. Fischer, A. Thess, R. E. Smalley, *Nature* **388**, 255 (1997).
15. L. Grigorian *et al.*, *Phys. Rev. Lett.* **80**, 5560 (1998).
16. M. S. Dresselhaus, G. Dresselhaus, P. C. Eklund, *Science of Fullerenes and Carbon Nanotubes* (Academic Press, New York, 1996).
17. D. Seyferth, *Acc. Chem. Res.* **5**, 65 (1972).
18. R. C. Haddon, S. V. Chichester, S. M. Stein, J. H. Marshall, A. M. Mujsce, *J. Org. Chem.* **52**, 711 (1987).
19. M. Tsuda, T. Ishida, T. Nogami, S. Kurono, M. Ohashi, *Tetrahedron Lett.* **34**, 6911 (1993).
20. J. Osterodt and F. Vogtle, *Chem. Commun.* (1996), p. 547.
21. D. V. Preda and L. T. Scott, *Chem. Eng. News*, 46 (13 April 1998), p. 46.
22. V. H. Crespi, M. L. Cohen, A. Rubio, *Phys. Rev. Lett.* **79**, 2093 (1997).

23. Supported by NSF Experimental Program to Stimulate Competitive Research grant EPS-9452895.

29 July 1998; accepted 31 August 1998

Ammonia Synthesis at Atmospheric Pressure

George Marnellos and Michael Stoukides

Ammonia was synthesized from its elements at atmospheric pressure in a solid state proton (H^+)–conducting cell-reactor. Hydrogen was flowing over the anode and was converted into protons that were transported through the solid electrolyte and reached the cathode (palladium) over which nitrogen was passing. At 570°C and atmospheric pressure, greater than 78 percent of the electrochemically supplied hydrogen was converted into ammonia. The thermodynamic requirement for a high-pressure process is eliminated.

The development of a successful process for ammonia synthesis from its elements:

$$N_2 + 3H_2 \leftrightarrow 2NH_3 \qquad (1)$$

is considered a landmark in heterogeneous catalysis. The Haber process, which involves reaction of gaseous nitrogen and hydrogen on an Fe-based catalyst at high pressures (15 to 30 MPa), was developed at the beginning of the 20th century after an extensive search for an active catalyst (*1*). Even from early studies, it was realized that the conversion is limited by thermodynamics. The gas volume decreases with reaction; hence, very high pressures must be used to push equilibrium to the right in reaction 1 according to the Le Chatelier principle. The reaction is exothermic (109 kJ/mol at 500°C), and therefore conversion increases with decreasing temperature. However, to achieve industrially acceptable reaction rates, the reaction temperature must be high. The trade-off solution is to operate at temperatures in the range of 430° to 480°C, at which the equilibrium conversion is on the order of 10 to 15% (*1*).

Despite the very high pressures used and the thermodynamically limited conversion, the Haber process remains after almost a century the dominant route to NH_3 synthesis, a key chemical produced at amounts on the order of 10^8 metric tons per year. We report on an alternative route to ammonia synthesis at atmospheric pressure through the use of solid state proton (H^+) conductors by which the requirement for operation at high pressures is eliminated.

Solid electrolyte cells have been used so far in heterogeneous catalysis to (i) study the mechanism of catalytic reactions (*2, 3*), (ii) electrochemically alter reaction rates (*4, 5*), and (iii) cogenerate electricity and useful chemicals (*6*). The solid electrolytes used in most of the above applications were oxygen ion conductors. In the last decade, however, materials that exhibit protonic conductivity in the solid state have been introduced into catalysis research (*7*). These H^+ conductors are particularly useful because they can operate at temperatures in which many industrial hydro- and dehydrogenation reactions take place. Furthermore, in contrast to oxidation reactions, a number of industrial hydrogenations (ammonia and methanol production) are equilibrium limited at the operating conditions.

A model process that uses solid state proton conductors to obtain conversions higher than those predicted by the reaction equilibrium has previously been proposed (*8*). The principle is as follows. Gaseous H_2 passing over the anode of the proton-conducting cell-reactor, will be converted to H^+:

$$3H_2 \rightarrow 6H^+ + 6e^- \qquad (2)$$

The protons (H^+) are transported through the solid electrolyte to the cathode where the half-cell reaction

$$N_2 + 6H^+ + 6e^- \rightarrow 2NH_3 \qquad (3)$$

takes place. Thus, reaction 1 is again the overall reaction. We have verified experimentally the above model process and present the results here.

A schematic diagram of the cell-reactor we used is shown in Fig. 1. It consisted of a nonporous ceramic tube (18 cm long, 1.25-cm inside diameter and 1.55-cm outside diameter) closed at the bottom end. The ceramic material was a strontia-ceria-ytterbia (SCY) perovskite of the form $SrCe_{0.95}Yb_{0.05}O_3$. This solid has good mechanical strength and high protonic conductivity (*9*). The ceramic tube was enclosed in a quartz tube (20 cm long, 3.60-cm inside diameter, and 4.10-cm outside diameter). Two porous polycrystalline palladium films were deposited on the inside and outside walls of the SCY tube and served as cathodic and anodic electrodes, respectively (Fig. 1). The solid state device constructed can be represented by the cell H_2, Pd | SCY | Pd, N_2, NH_3, He.

The electrode preparation and characterization procedure has been described in detail elsewhere (*10*). The superficial surface area of each electrode was 1.3 cm^2, and the true

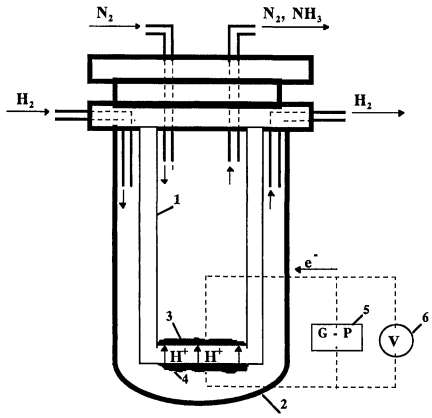

Fig. 1. Schematic diagram of the cell-reactor: 1, SCY ceramic tube (H^+ conductor); 2, quartz tube; 3, cathodic electrode (Pd); 4, anodic electrode (Pd); 5, galvanostat-potentiostat; and 6, voltmeter.

Chemical Engineering Department and Chemical Process Engineering Research Institute, Aristotle University of Thessaloniki, Thessaloniki 54006, Greece.

catalytic surface area of the cathode was about 80 cm^2. The cathode was exposed to a gaseous stream containing nitrogen diluted in helium and the anode was exposed to a hydrogen stream. The lower part of the cell-reactor was placed in a furnace where the temperature was controlled. The two electrodes were connected to a differential voltmeter as well as to a galvanostat-potentiostat by which the desired current was applied (Fig. 1).

Analysis of the inlet and outlet gas was performed by online gas chromatography (GC) with a molecular sieve 13X and a Porapak N column. In addition to ammonia measurements, we measured online the inlet and outlet N_2 concentrations at the cathode. From the imposed current, we could accurately determine the moles of hydrogen reaching the cathode per second. The moles of reacted hydrogen were calculated to be within ±3 to 5% of three times the moles of reacted nitrogen, that is, according to the stoichiometry of reaction 1.

In addition to the GC measurements, the gaseous outlet stream from the cathode was bubbled for about 1 hour through a flask that contained 75 ml of HCl with an initial pH of about 4.00. An electronic pH meter was used to measure the pH before and after the gas was passed through the flask. The difference in pH, converted into reacted HCl, was in very good agreement with the amount of NH_3 produced according to the GC measurements. Also, we did "blank" tests by bubbling the exit gas from the cathode for 1 hour through the flask with the cell operating under open-circuit conditions (current $I = 0$). There was no pH change in the blank tests. Finally, on several occasions, samples from the titration flasks were checked for ammonia content by using Nessler's reagent. The results were positive for the "closed-circuit" samples and negative for the blank samples.

The dependence of the rate of NH_3 formation and of hydrogen conversion, respectively, on $I/2F$, where I is the imposed current and F is Faraday's constant, is shown in Fig. 2. According to previous studies (*11, 12*), at the conditions we used ($I < 2$ mA/cm^2; temperature $T = 570$°C; 100% H_2 on one side, He-N_2 mixtures on the other side) the proton transference number must be very close to unity; therefore, the ratio $I/2F$ is equal to the electrochemical molar flux of hydrogen through the solid electrolyte. The cell was kept at 570°C. A mixture of 1.8% N_2 in He was passed over the cathode at a volumetric flow rate of 8.3×10^{-8} m^3/s and atmospheric total pressure. A flow of 5.0×10^{-7} m^3/s of 100% H_2 at atmospheric pressure was maintained over the anode. At $I = 0$, no products were formed. Upon imposing a current through the cell, NH_3 appeared at the cathode, and after a transient period of 2 to 6 min, a steady-state rate of NH_3 formation was established (Fig. 2A). The two dotted lines of Fig. 2A are based on thermodynamic calculations and compare the present results with those that would have been obtained in a conventional catalytic reactor (CCR) in which gaseous H_2 rather than electrochemical H^+ was used. The CCR is a hypothetical catalytic reactor in which all the reactants are gases, the inlet molar flow rates of nitrogen and helium are the same as in our cell-reactor, and the inlet molar flow rate of gaseous H_2 is equal to $I/2F$. We further assume that in the CCR, the residence time is so long and the catalyst so good that the exit molar flow rate of ammonia corresponds to thermodynamic equilibrium of reaction 1 at 570°C and atmospheric pressure. Hence, the CCR curve represents the maximum rate of NH_3 production that can be obtained in a conventional reactor. The NH_3 production rates attained experimentally exceed the CCR rates by at least three orders of magnitude. Similarly, the curve denoted as PCCR (pressure in a conventional catalytic reactor) represents the total pressure at which a CCR should operate in order for the NH_3 conversion to be as high as that reported here. The pressure values are on the order of 10^5 MPa (10^6 bar).

In Fig. 2B, the percent conversion of H_2 (100 multiplied by the moles of H_2 reacted divided by the moles of H_2 fed in) is plotted versus the rate of electrochemical supply of hydrogen, $I/2F$, and shows that H_2 is almost completely converted into NH_3. Again, the bottom dotted line corresponds to the maximum (equilibrium) conversion that could be attained in a CCR.

The corresponding conversion of N_2 into NH_3 was considerably lower. This difference was not due, however, to lower reactivity of N_2. In these experiments, H_2 was the limiting reactant and therefore the rates of NH_3 formation were very close to two-thirds the rates of H_2 supply, according to the stoichiometry of reaction 1. This point is better shown in Fig. 3 where the rate of production of NH_3 is plotted versus $I/2F$, for three different inlet partial pressures of N_2: 0.3, 1.0, and 1.8 kPa. The continuous straight line corresponds to 100% conversion of H_2 into NH_3. The reaction rate is essentially independent of the partial pressure of N_2. Also, for all N_2 pressures we examined, at least 78% of H_2 was converted into NH_3.

In addition to the difficulty of producing NH_3 from its elements, the success of a process also depends on the extent of the reverse reaction of NH_3 decomposition; ammonia does decompose in the gas phase. To diminish this effect, we designed the cell such that only the bottom of the SCY tube was at the temperature of operation whereas most of the tube was outside the furnace. The degree of NH_3 decomposition was quantitatively determined from experiments in which gaseous NH_3 was introduced together with N_2 at flow rates equal to those used in the NH_3 synthesis experiments. Indeed, we found that NH_3 decomposed into H_2 and N_2. Nevertheless, the measured decomposition was 20% or less.

In the present experiments, the limiting reactant was the electrochemically supplied hydrogen. A sixfold increase in N_2 partial pressure has essentially no effect on the rate of NH_3 formation (Fig. 3). To study intrinsic

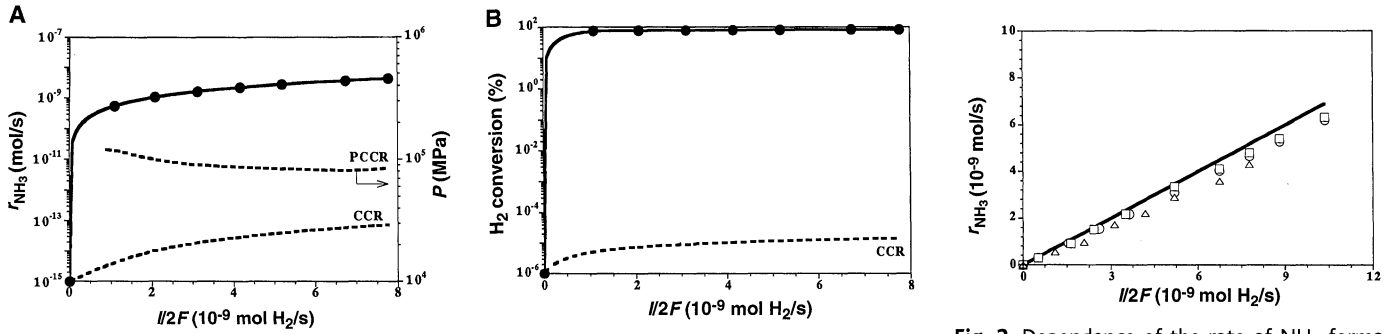

Fig. 2. Dependence of the rate of (**A**) NH_3 formation and of (**B**) the percent conversion of H_2 on the rate of electrochemical hydrogen supply, $I/2F$, under the following conditions: temperature, 570°C, and inlet partial pressure of N_2, 1.8 kPa. In (A), the CCR curve is the calculated NH_3 formation rate in a CCR and the PCCR curve is the calculated total pressure of operation of a CCR. In (B), the CCR curve is the calculated percent conversion of H_2 in a CCR.

Fig. 3. Dependence of the rate of NH_3 formation on the rate of electrochemical hydrogen supply $I/2F$ for three partial pressures of N_2: 0.3 kPa (circles), 1.0 kPa (squares), and 1.8 kPa (triangles) at 570°C. The continuous line represents complete conversion of H_2 into NH_3.

kinetics, we should increase considerably the current density. Nevertheless, this was not possible at 570°C because of the ohmic resistance of the SCY. We could obtain higher H^+ fluxes by increasing the temperature, but this would also increase the rate of NH_3 decomposition. Further work is needed to determine the optimum operating temperature, so to propose a mechanism at this stage would be primarily speculation.

This process offers an alternative route that permits operation at desired pressures and temperatures without the thermodynamic restrictions imposed on conventional catalytic reactors. The above experimental observations show that H_2 is quantitatively converted into NH_3 regardless of the thermodynamic restrictions for limited conversion. This result does not mean that the present data violate thermodynamics in any aspect. Simply, the final state of high conversion to NH_3 is achieved by the consumption of electrical work by the system. This situation is similar to the case of H_2O dissociation into H_2 and O_2: if this reaction is carried out at 25°C and atmospheric pressure, the thermodynamically calculated mole fractions of H_2 and O_2 at equilibrium are on the order of 10^{-27}. Nevertheless, water is quantitatively dissociated if electrical work is offered (electrolysis).

References and Notes

1. C. N. Satterfield, *Heterogeneous Catalysis in Practice* (McGraw-Hill, New York, 1980), pp. 301–308.
2. M. Stoukides, *Ind. Eng. Chem. Res.* **27**, 1745 (1988).
3. C. G. Vayenas, M. M. Jaksic, S. I. Bebelis, S. G. Neophytides, in *Modern Aspects in Electrochemistry*, J. O'.M. Bockris, B. E. Conway, W. R. E. White, Eds. (Plenum, New York, 1996), vol. 29, pp. 57–202.
4. T. M. Gür and R. A. Huggins, *Science* **219**, 967 (1983).
5. Y. Jiang, I. V. Yentekakis, C. G. Vayenas, *ibid.* **264**, 1563 (1994).
6. C. G. Vayenas and R. D. Farr, *ibid.* **208**, 593 (1980).
7. H. Iwahara, *Solid State Ionics* **86–88**, 9 (1996).
8. E. Panagos, I. Voudouris, M. Stoukides, *Chem. Eng. Sci.* **51**, 3175 (1996).
9. H. Iwahara, T. Esaka, H. Uchida, N. Maeda, *Solid State Ionics* **3–4**, 359 (1981).
10. C. Athanasiou, G. Marnellos, P. Tsiakaras, M. Stoukides, *Ionics* **2**, 353 (1996).
11. S. Hamakawa, T. Hibino, H. Iwahara, *J. Electrochem. Soc.* **140**, 459 (1993).
12. P.-H. Chiang, D. Eng, M. Stoukides, *Solid State Ionics* **61**, 99 (1993).

13. We thank P. Bekiaroglou for useful comments and suggestions. Supported by the Chemical Process Engineering Research Institute.

11 June 1998; accepted 21 August 1998

An *Arabidopsis* Mutant Defective in the Plastid General Protein Import Apparatus

Paul Jarvis, Lih-Jen Chen, Hsou-min Li, Charles A. Peto, Christian Fankhauser, Joanne Chory*

Elaborate mechanisms have evolved for the translocation of nucleus-encoded proteins across the plastid envelope membrane. Although putative components of the import apparatus have been identified biochemically, their role in import remains to be proven in vivo. An *Arabidopsis* mutant lacking a new component of the import machinery [translocon at the outer envelope membrane of chloroplasts (Toc33), a 33-kilodalton protein] has been isolated. The functional similarity of Toc33 to another translocon component (Toc34) implies that multiple different translocon complexes are present in plastids. Processes that are mediated by Toc33 operate during the early stages of plastid and leaf development. The data demonstrate the in vivo role of a translocon component in plastid protein import.

The routing of newly synthesized proteins to appropriate subcellular compartments is a fundamental process that is common to all organisms. In plants, chloroplasts (the photosynthetic plastids of green tissues) are the major target of such protein trafficking because they account for >50% of the total soluble protein in leaves and because >80% of the proteins required for their formation are encoded in the nucleus (*1*). The translocation of proteins across the envelope membrane is especially important early on in chloroplast and leaf development, when the photosynthetic apparatus is being assembled for the establishment of photoautotrophic growth (*1*). The capacity of plastids to import proteins is regulated developmentally and is maximal during these early stages of organ expansion (*2*).

Genetic screens for loci affecting the expression of nucleus-encoded photosynthetic proteins have identified several mutants with defects in plastid biogenesis (*3, 4*). Here, we describe a new mutant, initially referred to by the number 127-4, which belongs in this category. The 127-4 mutant was identified as having a recessive, pale phenotype in a population of transferred DNA (T-DNA)–mutagenized plants. Although the mutant appeared uniformly pale during the first 2 weeks of its life cycle (Fig. 1, A and B), the oldest leaves of mature plants frequently had an appearance closer to that of the wild type (Fig. 1C) (*5*).

P. Jarvis and C. Fankhauser, Plant Biology Laboratory, Salk Institute, 10010 North Torrey Pines Road, La Jolla, CA 92037, USA. L.-J. Chen and H.-m. Li, Institute of Molecular Biology, Academia Sinica, Nankang, Taipei 11529, Taiwan. C. A. Peto, Laboratory of Neuronal Structure and Function, Salk Institute, 10010 North Torrey Pines Road, La Jolla, CA 92037, USA. J. Chory, Plant Biology Laboratory and Howard Hughes Medical Institute, Salk Institute, 10010 North Torrey Pines Road, La Jolla, CA 92037, USA.

*To whom correspondence should be addressed. E-mail: chory@salk.edu

The gene disrupted by the T-DNA insertion (Fig. 2A) encodes a 33-kD protein that is very similar to Toc34 from *Arabidopsis* (61% amino acid identity) and pea plants (59% amino acid identity) (Fig. 2B); *Arabidopsis* Toc34 and pea Toc34 share 64% amino acid identity (*6–8*). Toc34 is a guanosine triphosphate (GTP)–binding protein of the plastid outer envelope membrane. Toc34, Toc75, and Toc86 are components of the outer envelope segment of the general import apparatus through which the majority of proteins destined for the plastid are believed to pass (*9*). The involvement of Toc34 in protein import is inferred from its interaction with preproteins during import and from its association with Toc75 and Toc86 (*10*). However, its precise role in the import process is not known. The 127-4 mutant was named *ppi1* (for plastid protein import), but we will refer to the protein encoded by the *PPI1* gene as Toc33, in accordance with biochemical nomenclature (*11*). The size (an estimated 13 kb) and location (in intron 2) of the T-DNA insertion, combined with our failure to detect any mRNA in mutant plants (*12*), indicated that the *ppi1* mutation was most likely null.

Given their strong sequence similarity, we tested the hypothesis that Toc33 and Toc34 might correspond to functionally equivalent translocon components. In vitro transcribed and translated Toc33 protein was found to insert itself into the outer envelope membrane of isolated pea chloroplasts in a similar manner to *Arabidopsis* Toc34 (*12, 13*), which suggests that the two proteins are similarly localized in vivo. We subsequently overexpressed Toc33 and Toc34 cDNA clones in *ppi1* plants and found that either protein could complement the chlorophyll deficiency of *ppi1*, which confirms the functional similarity of the two proteins (Fig. 2C) (*14, 15*). The existence of two functionally similar Toc proteins suggests that at least two distinct translocon complexes exist in *Arabidopsis*. This observation is of particular